## Supporting Information

# Production of Renewable Oleo-Furan Surfactants by Cross-Ketonization of Biomass-Derived Furoic Acid and Fatty Acids

Hannah Nguyen,[a] Yunzhu Wang,[b] David Moglia,[a] Jiayi Fu,[a,b] Weiqing Zheng,[b] Marat Orazov*[a,b] and Dionisios G. Vlachos*[a,b]

[a] *Department of Chemical and Biomolecular Engineering, University of Delaware, Newark, Delaware 19716, USA*

[b] *Catalysis Center for Energy Innovation, Newark, Delaware 19716, USA.*

*Email: orazov@udel.edu; vlachos@udel.edu*

## Thermochemistry calculations

a. Acylation of furan with acetic anhydride

All ΔG calculations were done at the G4 level

Furan:acetic anhydride molar ratio = 1:1

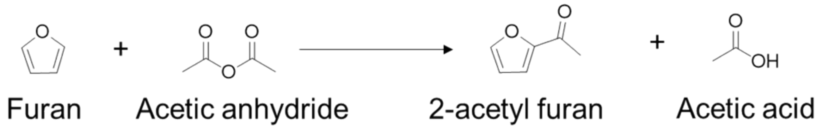

| Temp (° C) | ΔG (T) (kcal/mol) | $K_{eq}$ | Furan Conversion (%) |
|---|---|---|---|
| 150 | -4.65 | 253.58 | 94.09 |
| 200 | -4.58 | 130.14 | 91.94 |
| 250 | -4.50 | 75.87 | 89.70 |

b. Acylation of furan with acetic acid or lauric acid
All ΔG calculations were done with m062-x functional and 6-311G(2df,β) basis set
Furan:acid molar ratio = 1:1

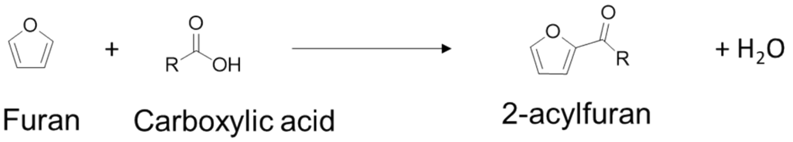

| Temp (° C) | ΔG (T) (kcal/mol) | | $K_{eq}$ | | Furan Conversion (%) | |
|---|---|---|---|---|---|---|
| | Acetic | Lauric | Acetic | Lauric | Acetic | Lauric |
| 150 | 10.81 | 11.31 | 2.59e-6 | 1.42e-6 | 0.16 | 0.12 |
| 200 | 10.97 | 11.48 | 8.75e-6 | 4.92e-6 | 0.29 | 0.22 |
| 250 | 11.07 | 11.65 | 2.35e-5 | 1.34e-5 | 0.48 | 0.37 |

c. Cross-ketonization of 2-furoic acid with acetic acid
All ΔG calculations were done at the G4 level
Furoic acid:acetic acid molar ratio = 1:1

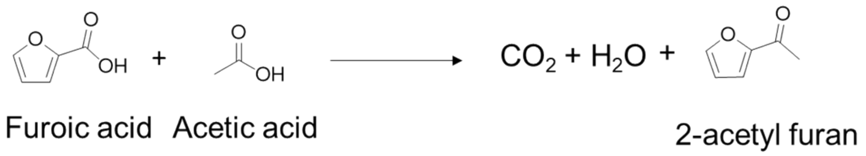

| Temp (° C) | ΔG (T) (kcal/mol) | $K_{eq}$ (M) | Furoic acid conversion |
|---|---|---|---|
| 150 | -14.1823 | 2.11E+07 | 100 |
| 200 | -15.8396 | 2.07E+07 | 100 |
| 250 | -17.4912 | 2.03E+07 | 100 |

## Calibration

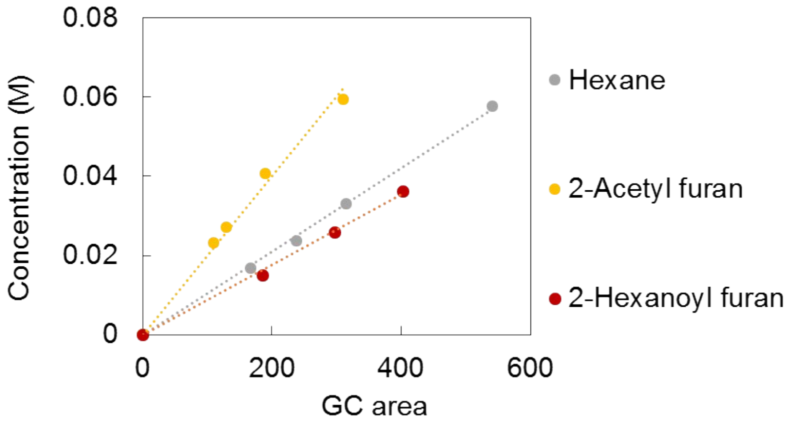

Figure S.1. GC calibration curves for chemical standards (●) hexane, (●) 2-acetyl furan, and (●) 2-hexanoyl furan.

Table S.1. Effective carbon number calculation for 2-dodecanoyl furan.

| Compound | Compound structure | Number of C | Calibrated slope | Theoretical slope | Effective carbon |
|---|---|---|---|---|---|
| **hexane** | 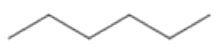 | 6 | 1.05E-04 | N/A | 6 |
| **2-acetyl furan** | 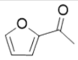 | 6 | 2.00E-04 | N/A | 3.15 |
| **2-hexanoyl furan** | 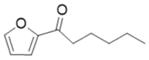 | 10 | 8.83E-05 | 8.83E-05 | 7.15 |
| **2-dodecanoyl furan** | 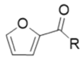<br>R = n-$C_{11}$ | 16 | N/A | 4.80E-05 | 13.15 |

## Catalyst screening at 300 °C

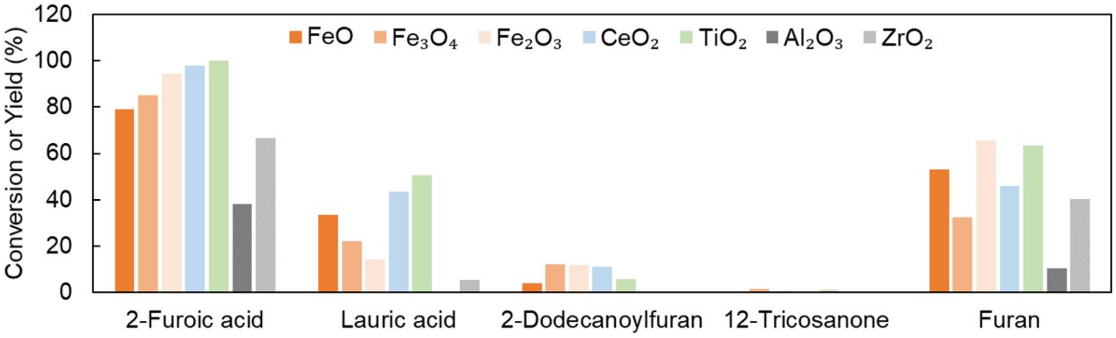

Figure S.2. Performance of various commercial metal oxides in the reaction of 2-furoic acid with lauric acid in n-dodecane. Reaction conditions: 0.05 M lauric acid, 0.25 M 2-furoic acid, 0.2 g catalyst, 300 °C, 90 min, 20 bar $N_2$, 800 rpm. The pressure at reaction temperature is 40 bar.

## Tests at various FA:LA ratios

The activity, at various lauric:acid molar ratios over $Fe_3O_4$, as a case study catalyst, suggests that the cross-ketonization is favored as higher furoic acid:lauric acid ratios (Figure S.3); therefore a lauric acid:furoic acid molar ratio of 1: 5 was chosen for the initial screening.

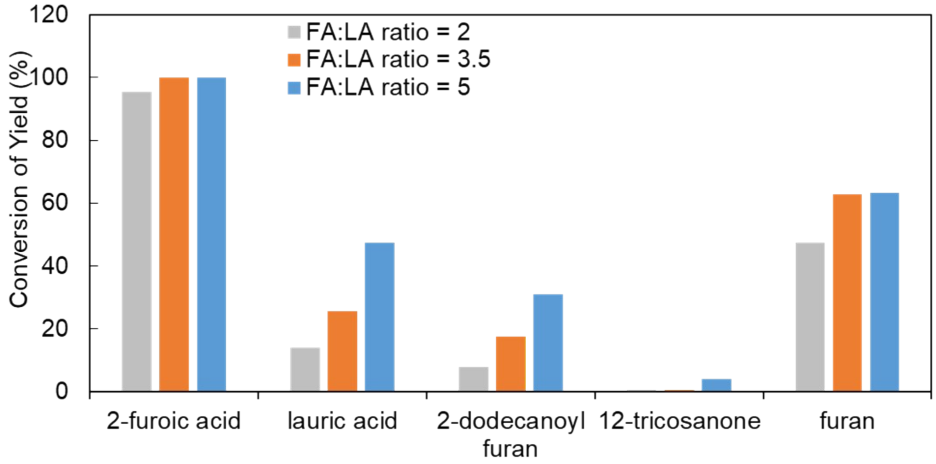

Figure S.3. Acid conversion and product yield at various furoic acid (FA) to lauric acid (LA) molar ratios, with the LA concentration constant at 0.05 M over the $Fe_3O_4$ catalyst. Reaction conditions: 0.05 M lauric acid, [0.1-0.25] M 2-furoic acid, 0.2 g $Fe_3O_4$, 316 °C, 90 min.

## External mass transfer tests

The activity (demonstrated for FeO) vs. the stirring speed from 600 to 1000 rpm, shown in Fig. S.4, indicates no external mass transfer limitations.

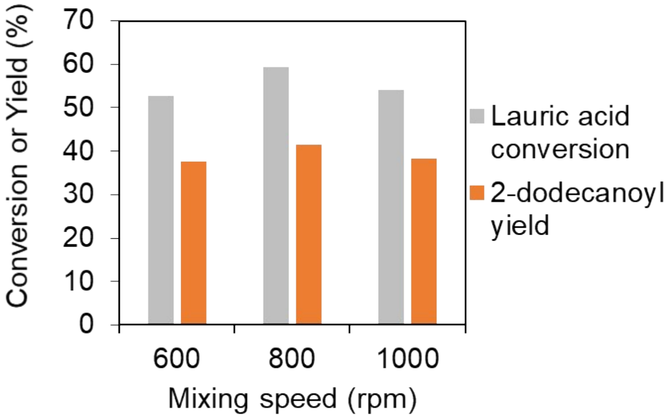

Figure S.4. Lauric acid conversion and 2-dodecanoyl yield at various mixing speeds. Reaction conditions: 0.05 M lauric acid, 0.25 M 2-furoic acid, 0.2 g FeO, 316 °C, 90 min.

## Carbon balance analysis

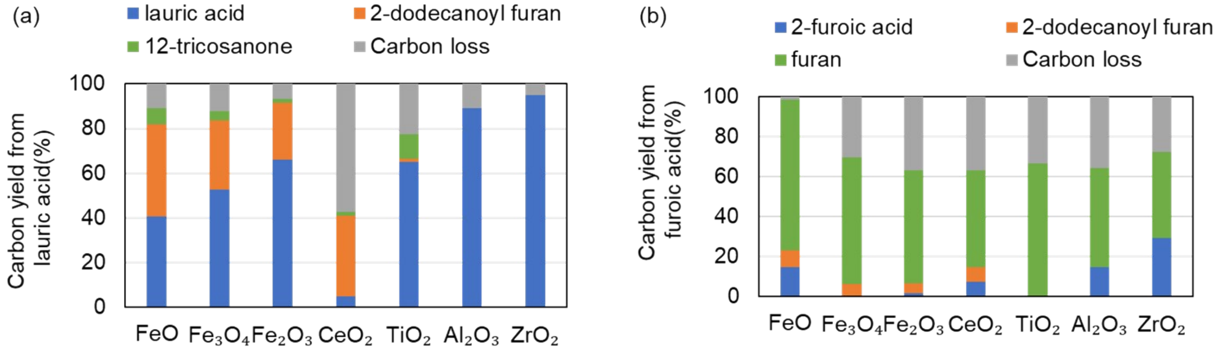

Figure S.5. Carbon balance for lauric acid and furoic acid in the catalyst screening experiments. Reaction conditions: 0.05 M lauric acid, 0.25 M 2-furoic acid, 0.2 g catalyst, 316 °C, 90 min, 20 bar $N_2$, 800 rpm.

## Activity of the homogeneous Fe species

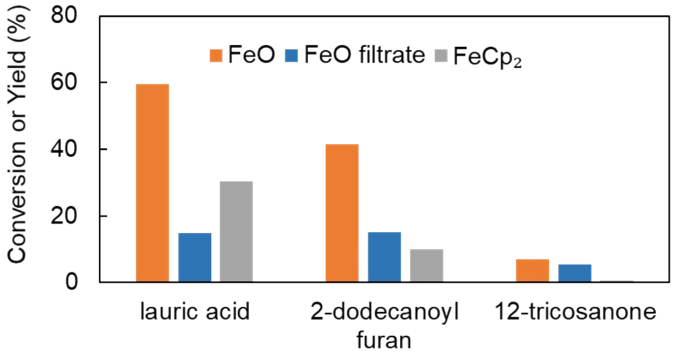

Figure S.6. Comparison of activity for cross-ketonization between FeO, its filtrate after the reaction, and homogeneous ferrocene ($FeCp_2$). Reaction conditions: 0.05 M lauric acid, 0.25 M 2-furoic acid, 0.2 g FeO or $FeCp_2$, 316 °C, 90 mins.

## Fe leaching test

Table S.2. Fe content in pure dodecane and post-reaction filtrates of iron oxides measured by ICP.

| | **FeO** | **$Fe_2O_3$** | **$Fe_3O_4$** |
|---|---|---|---|
| **Run 1** | 70 ppm | 10 ppm | 10 ppm |
| **Run 2** | 35 ppm | 15 ppm | 12 ppm |
| **Run 3** | 94 ppm | 14 ppm | 9 ppm |
| **Dodecane** | 10 ppm | | |

The Fe concentration detected in the post-reaction filtrates of $Fe_3O_4$ and $Fe_2O_3$ is comparable to that of pure dodecane, indicating that the Fe species are at the measurement noise level.

## Reduction profile of the $Fe_xO_y$ catalysts

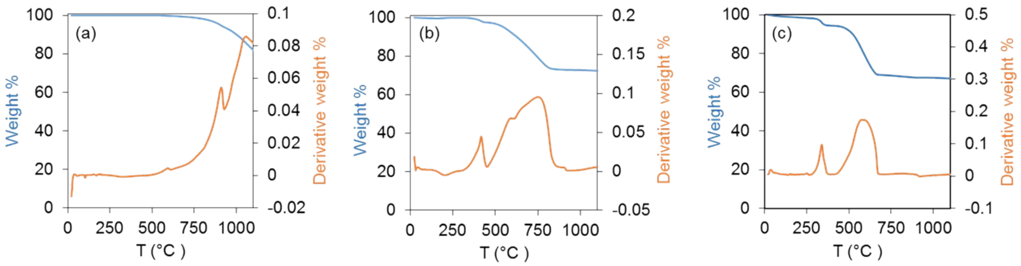

Figure S.7. $H_2$ TPR-TGA profiles of iron oxides: FeO (a), $Fe_3O_4$ (b), and $Fe_2O_3$ (c).

## Induction period in catalyst activity

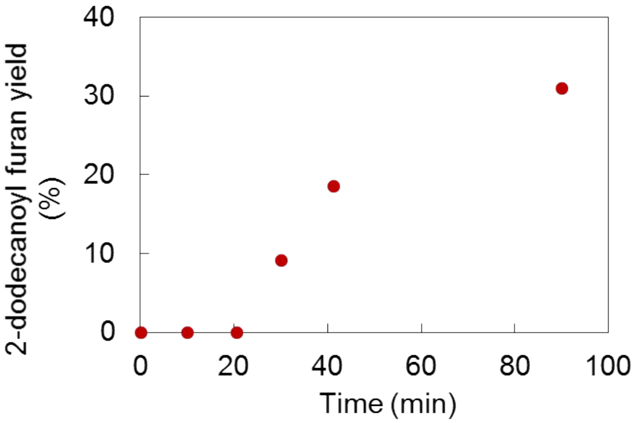

Figure S.8. Time evolution of 2-dodecanoyl furan formation over $Fe_3O_4$. Reaction conditions: 0.05 M lauric acid, 0.25 M 2-furoic acid, 0.2 g $Fe_3O_4$, 316 °C.

## Oxidation state of Fe of the surface of $Fe_3O_4$

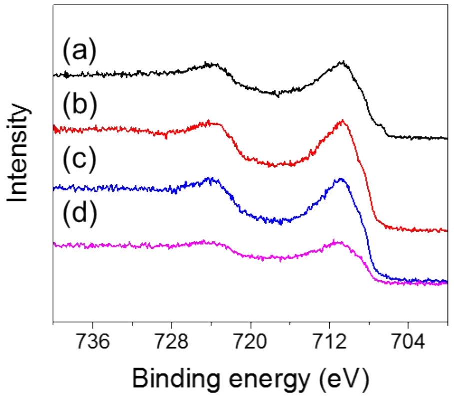

Figure S.9. XPS spectra of Fe $2p_{3/}$ of $Fe_3O_4$ catalyst pretreated in $H_2$ (a), pure dodecane (b), 0.05 M lauric acid in dodecane (c), and 0.25 M furoic acid in dodecane (d). Reaction conditions: 0.2 g $Fe_3O_4$, 316 °C, 30 min.

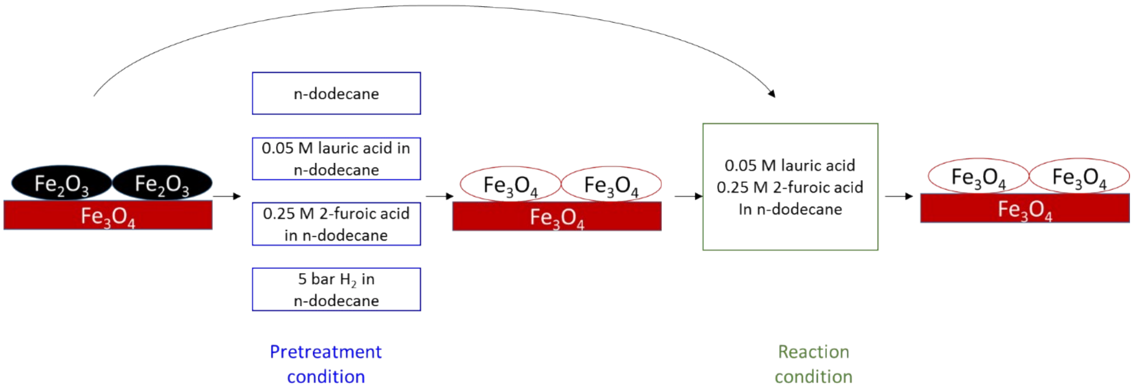

Figure S.10. Iron oxidation state on the surface of $Fe_3O_4$ before and after pretreatment and reaction as shown by XPS.

## Acidity measurement of the fresh oxides

Pyridine Fourier transform infrared (FT-IR) spectroscopy was conducted on an FT-IR Spectrometer (Nicolet 8700) equipped with a MCT detector (128 scans at a spectral resolution of 2 $cm^{-1}$ ). The catalyst sample was pressed to a thin pellet before analysis. FeO, $Fe_2O_3$, $Fe_3O_4$, or $CeO_2$ was mixed with $SiO_2$ at a mass ratio of 1:4 before being pressed. The pellet was heated to 300 °C for 1 h under vacuum of approximately $10^{-5}$ Pa to remove adsorbed water and impurities. The sample was then cooled to 150 °C, at which the background was scanned. Pyridine (>99%, Sigma Aldrich) was adsorbed on the sample for 10 min. The sample was then evacuated under vacuum for 20 min, and the spectra were collected.

The peaks corresponding to Lewis acid sites and Brønsted acid sites are labeled as LS and BS, respectively, in Figure S.11 below.

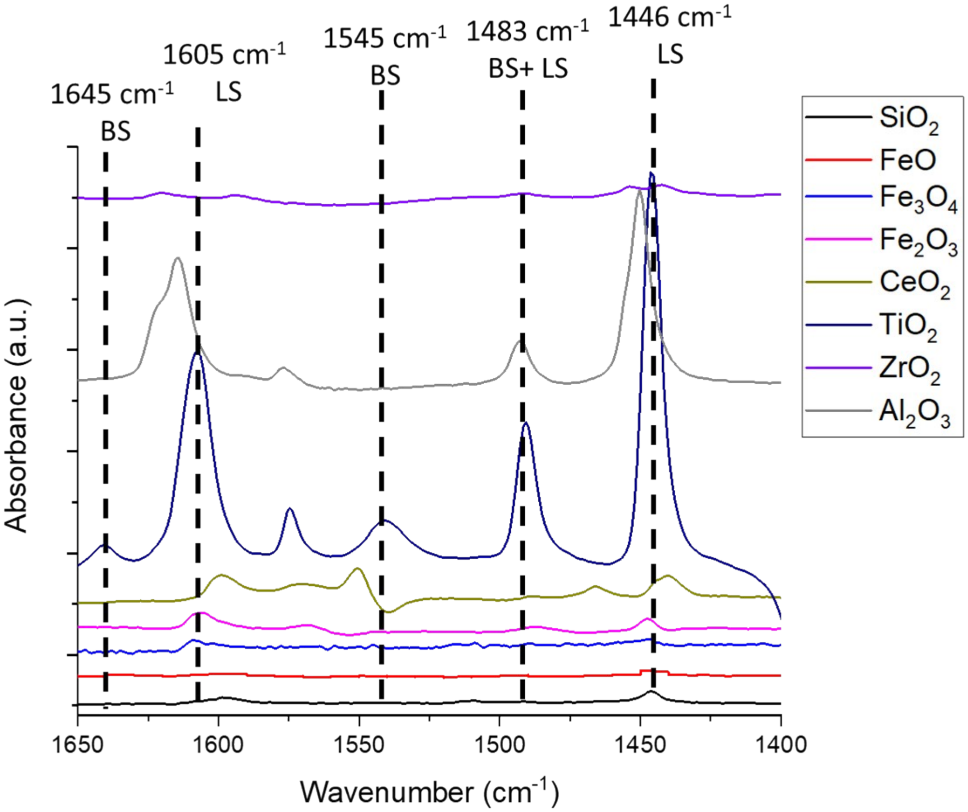

Figure S.11. IR spectra of pyridine adsorption on the fresh metal oxide catalysts.

## Isostopic tracing

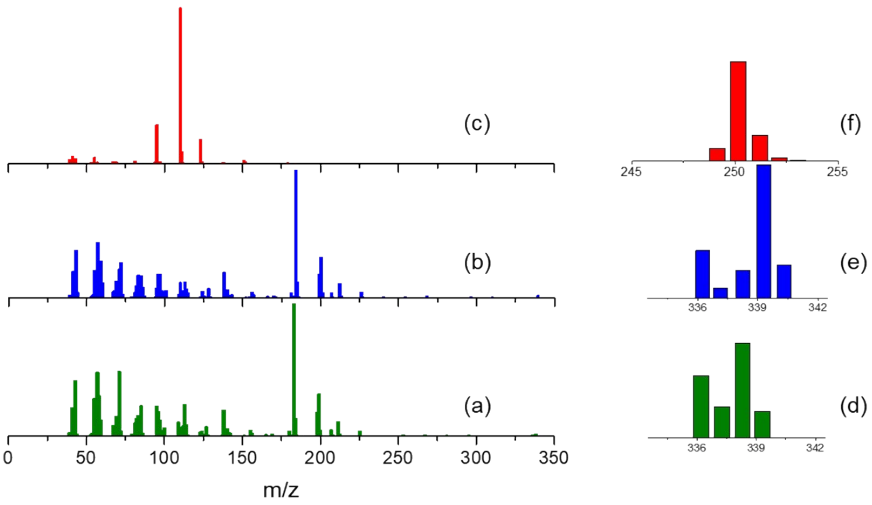

Figure S.12. GCMS spectra of (a) 12-tricosanone from reaction starting with unlabeled lauric, (b) 12-tricosanone from reaction starting with $^{13}$C-C1 lauric acid, and (c) 2-dodecanoyl furan from reaction starting with$^{13}$C-C1 lauric acid, and their respective zoomed in region in (d), (e), and (f).

## $N_2$ physisorption data of the catalysts

Table S.3. BET surface areas and micropore volumes of fresh oxide catalysts and the spent iron oxides after cross-ketonization reactions.

| | **Fresh catalyst** | | | | | | | **Spent catalyst** | | |
|---|---|---|---|---|---|---|---|---|---|---|
| | **FeO** | **$Fe_3O_4$** | **$Fe_2O_3$** | **$CeO_2$** | **$TiO_2$** | **$Al_2O_3$** | **$ZrO_2$** | **FeO** | **$Fe_3O_4$** | **$Fe_2O_3$** |
| **BET surface area ($m^2/g$)** | 0.1 | 8.8 | 34.3 | 75.4 | 84.5 | 79.0 | 104.5 | 18.7 | 9.1 | 17.7 |
| **Micropore volume ($cm^3/g$)** | 2.83e-4 | 2.18e-2 | 7.58e-2 | 0.23 | 0.27 | 0.33 | 0.62 | 8.43e-2 | 2.29e-2 | 8.53e-2 |